

Theoretical Analysis of a Carbon-Carbon Dimer Placement Tool for Diamond Mechanosynthesis

Ralph C. Merkle,^{*,†} and Robert A. Freitas, Jr.[‡]

Zyvex Corp., 1321 North Plano Road, Richardson, Texas, USA

Density functional theory is used with Gaussian 98 to analyze a new family of proposed mechanosynthetic tools that could be employed for the placement of two carbon atoms—a carbon-carbon (CC) dimer—on a growing diamond surface at a specific site. The analysis focuses on specific group IV-substituted biadamantane tool tip structures and evaluates their stability and the strength of the bond they make with the CC dimer. These tools should be stable in a vacuum and should be able to hold and position a CC dimer in a manner suitable for positionally controlled diamond mechanosynthesis at room temperature.

Keywords: Adamantane, Carbon, Density Functional Theory, Diamond, Dimer, Mechanosynthesis, Nanotechnology, Positional Control.

1. INTRODUCTION

Arranging atoms in most of the ways permitted by physical law is a fundamental objective of nanotechnology. A more modest and specific objective is the ability to synthesize a wide range of stiff hydrocarbons—including molecularly precise diamond structures—with the use of positionally controlled molecular tools. Such positional control might be achieved with an instrument like a scanning probe microscope (SPM). Several theoretical proposals for molecular tools have already been made.^{1–4} For example, the theoretical proposal of Drexler² for a hydrogen abstraction tool appears feasible, based on the *ab initio* investigations of Musgrave et al.,¹ the molecular mechanics investigations of Sinnott et al.⁵ and Brenner et al.,⁶ and other theoretical work.^{7–10} Previous proposals for various carbon deposition tools^{2,3} have not yet been extensively explored theoretically.^{4,11}

In this paper, we propose and analyze new tools that might be useful in the precise placement of two carbon atoms (a carbon dimer) on a growing molecular structure. Two carbon atoms held together by a triple bond can—for many purposes—be treated as a single unit: a dimer. The function of a dimer placement tool is to position the dimer, then to bond the dimer to a precisely chosen location on a growing molecular structure, and finally to withdraw the tool—leaving the dimer behind on the growing structure. To achieve this, the dimer is required to be (1) bonded relatively weakly to the tool and (2) highly

strained and thus highly reactive so it will easily bond to the growing molecular structure to which it is added.

There is a large combinatorial space of possible tools that might satisfy both requirements. For those tools that are modeled here, we attempt to satisfy the two basic requirements by bonding the dimer to two group IV supporting atoms: carbon, silicon, germanium, tin, or lead. This series of elements forms progressively weaker bonds with carbon, so the proposed tools will likewise be progressively more weakly bound to the carbon-carbon (CC) dimer. The supporting group IV atoms are part of two substituted adamantane (C₁₀H₁₆) frameworks that position and orient them. The two substituted adamantane¹² frameworks are rotated and fused together to make a biadamantane¹³ structure (Fig. 1), creating very high-angle strain in the bonds between the two supporting atoms and the dimer. This molecule, a bi-silaadamantane dicarbon, is only the tip of a complete tool. In a complete mechanosynthetic apparatus, a somewhat larger version of this molecule would likely be required, so that the active tip could be held and positioned via a rigid handle structure.

Three basic tool tip configurations are readily apparent (Fig. 2): a dicarbon bridge (DCB) motif (the subject of this paper) in which each Si atom is bound to two central carbon bridges, a monocarbon bridge (MCB) motif in which each Si atom is bound to a central bridge of two carbon atoms in the tool, and a “chevron” motif.

The aspect ratio of the dimer placement tool may be increased by substituting two five-member rings at each shoulder of the tool tip (e.g., DCB5, MCB5) in place of the six-member rings (DCB6, MCB6), which more closely resemble the bulk diamond (lonsdaleite) handle structure, thus slightly elevating the carbon dimer above

*Author to whom correspondence should be addressed.

[†]Mailing Address: 1134 Pimento Ave., Sunnyvale, CA 94087, USA.

[‡]Mailing Address: P.O. Box 605, Pilot Hill, CA 95664, USA.

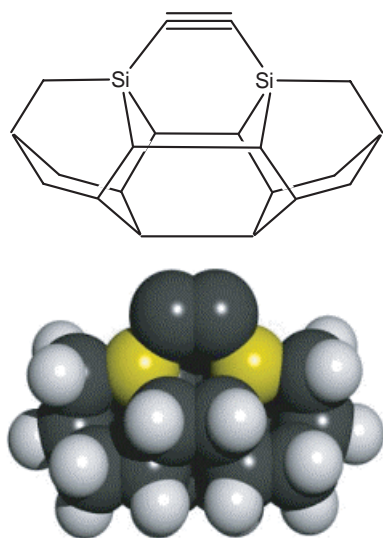


Fig. 1. DCB6-Si dimer placement tool tip.

the top of the shoulder at the cost of increased tip structure strain. Other details of the tip structure can also be varied. For example, the two group IV supporting atoms could be replaced with two group V elements, allowing the

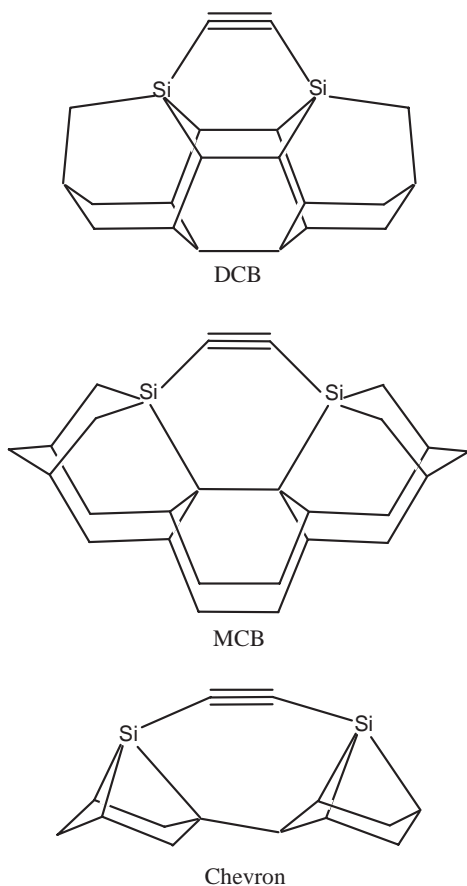


Fig. 2. Dimer placement tool tips based on dicarbon bridge (DCB), monocarbon bridge (MCB), and “chevron” motifs.

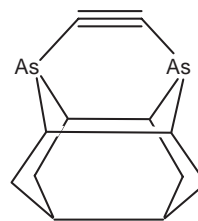


Fig. 3. DCB-As configuration of dimer placement tool tip.

shoulder atoms to be removed entirely—which increases the tool tip aspect ratio but may decrease the tool tip rigidity (Fig. 3). These and other tool tip structures that might be useful, along with the methods by which this family of tool tips might be chemically synthesized and then bound to an SPM tip, and spent tool tips recharged, will be described in future work.

Density functional theory (DFT) analysis suggests that the group IV-substituted adamantane-derived framework of highly reactive tools should be stable in vacuum prior to interacting with any surface and remains relatively weakly bonded to the dimer while still orienting the dimer appropriately. Each desired tool structure is a minimum on the potential energy surface (PES). Most possible undesired alternative tool structures are transition states or are not even stationary points on the PES, though one tool variant considered here (DCB6-C) has an unusually shallow minimum on the PES.

Here we investigate this proposed new class of horizontal dimer placement tools by focusing on the six particular tool tip structures shown in Figure 4, evaluating both their stability and the strength of their bonding to the CC dimer.

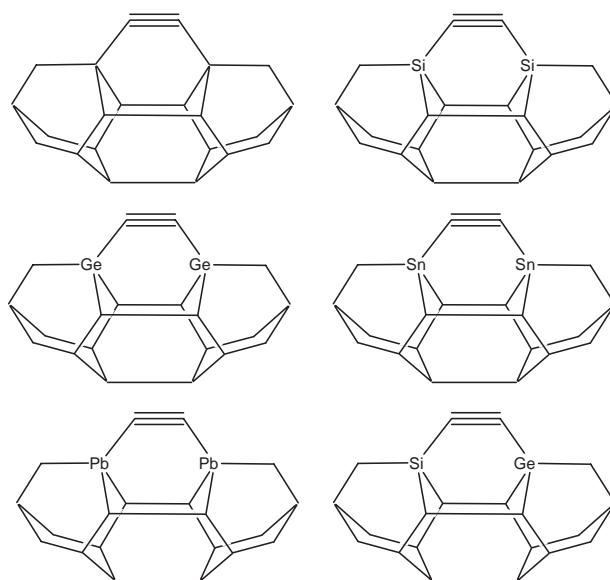


Fig. 4. Six mechanosynthetic tool tip variants for dimer placement tools (DCB6-C, DCB6-Si, DCB6-Ge, DCB6-Sn, DCB6-Pb, and DCB6-SiGe).

2. EXPERIMENTAL DETAILS

All six tool tip structures were evaluated with DFT in Gaussian 98.¹⁴ Geometries involving carbon, silicon, and germanium supporting atoms were optimized with the B3LYP/3-21G* level of theory unless otherwise noted. Geometries involving tin and lead supporting atoms were optimized with B3LYP/LANL2DZ. The LANL2DZ basis set is specialized for dealing with high Z atoms (beyond the third row). The stability of the wave functions was verified with the use of the STABLE keyword, and the nature of the stationary point was verified with the use of a frequency calculation in all cases. Single-point calculations at the B3LYP/6-311 + G(2d,p) level of theory were used for energy calculations for structures with carbon, silicon, and germanium supporting atoms.

The accuracy of B3LYP/6-311 + G(2d,p)//B3LYP/3-21G* energies should be adequate for the purposes considered here. A slightly lower level of theory (in which the geometry is optimized at HF/3-21G*) has a mean absolute deviation of 0.14 eV.¹⁵ We would expect that the slightly better level of theory used here would not have a worse mean absolute deviation. Thermal noise at room temperature is about 0.02 eV; in conventional positionally uncontrolled chemistry, errors on the order of 0.14 eV might well influence reaction rates and the dominant reaction pathway taken when multiple alternative reaction pathways are present. However, in the context of the present analysis this should not be an issue because alternative reaction pathways are limited by the use of positional control. Encounters between the reactive tool tip and the growing workpiece take place only at the desired position and only in the desired orientation. Alternative pathways that might otherwise occur in solution when molecules encounter each other in multiple random orientations and positions are largely eliminated by this approach. In addition, we would expect that the relative accuracy of the very similar structures compared here would be significantly better than the absolute errors generated by comparison of dissimilar structures¹⁵—the mean absolute deviation is computed from structures that are sometimes quite different.

The accuracy of the B3LYP/LANL2DZ level of theory has not been as extensively investigated. However, it is commonly used for studies of high Z atoms.¹⁵

3. RESULTS AND DISCUSSION

3.1. Stationary Points and Rearrangements

The results of tool tip energy calculations are summarized in Table I.

Figure 5 shows the three stationary points of primary interest: (A) the dimer placement tool with attached dimer, (B) the undesired carbenic rearrangement of the basic tool, and (C) the tool after placement of the dimer

Table I. Energy calculations for dimer placement tool molecules having group IV atoms used as attachment points for CC dimer.

Tool tip configuration	Energy (eV)
DCB6-C	-23197.52
Carbene rearrangement	-23197.15 (diff: 0.37)
Discharged DCB6-C	-21123.60
CC	-2065.32
CC + discharged DCB6-C	-23188.93
Minus DCB6-C	8.59
DCB6-Si	-36882.22
Carbene rearrangement	-36881.26 (diff: 0.96)
Discharged DCB6-Si	-34808.11
CC	-2065.32
CC + discharged DCB6-Si	-36873.43
Minus DCB6-Si	8.79
DCB6-SiGe	-85522.11
Discharged DCB6-SiGe	-83448.49
CC dimer	-2065.32
CC + discharged DCB6-SiGe	-85513.81
Minus DCB6-SiGe	8.30
DCB6-Ge	-134161.98
Carbene rearrangement	-134161.12 (diff: 0.86)
Discharged DCB6-Ge	-132088.86
CC dimer	-2065.32
CC + discharged DCB6-Ge	-134154.18
Minus DCB6-Ge	7.80
DCB6-Sn	-21298.01
Carbene rearrangement	-21297.27 (diff: 0.74)
Discharged DCB6-Sn	-19226.27
CC dimer	-2064.49
CC + discharged DCB6-Sn	-21290.76
Minus DCB6-Sn	7.25
DCB6-Pb	-21301.01
Carbene rearrangement	-21300.36 (diff: 0.65)
Discharged DCB6-Pb	-19230.37
CC dimer	-2064.49
CC + discharged DCB6-Pb	-21294.86
Minus DCB6-Pb	6.15
Singlet/triplet energy gap	
DCB6-Si	3.44
Carbene rearrangement	2.92

DCB6-C, DCB6-Si, DCB6-SiGe, DCB6-Ge: Energies computed at B3LYP/6-311 + G(2d,p)//B3LYP/3-21G* (single point at B3LYP/6-311 + G(2d,p) with zero-point correction from a frequency calculation at the B3LYP/3-21G* level of theory) for structures all of whose heavy atoms are C, Si, or Ge.

DCB6-Sn, DCB6-Pb: Energies computed at B3LYP/LANL2DZ (with zero point correction at the same level of theory) for all structures which include Sn or Pb atoms.

DCB6-Si singlet/triplet gap:- Triplet energies computed at B3LYP/6-311 + G(2d,p) triplet//B3LYP/3-21G* singlet (without zero point correction).

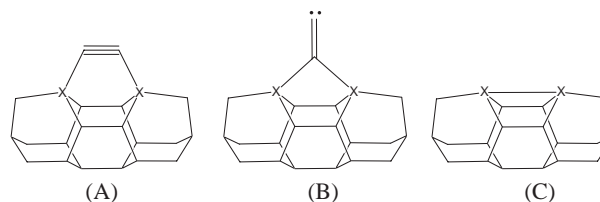


Fig. 5. Stationary points of interest for DCB6-X dimer placement tool analysis.

and after tool withdrawal from the surface. The element X can be carbon, silicon, germanium, tin, or lead. Other possibilities for X have not been investigated for this paper. The left and right instances of X can be different elements if asymmetrical tool properties are desired, though we have considered only a single example of this possibility here. Note that points A, B, and C represent states of the tool in isolation, and we do not consider interactions with a diamond surface. The present paper focuses purely on the tool and possible pathologies that could rule out its use. Analysis of tool-surface interactions is expected to require significant further effort and will be the subject of a future paper.

For almost all choices of X investigated here, the undesired carbenic rearrangement is a transition state on the potential energy surface—a frequency analysis of the stationary point shows one imaginary frequency—while both the tool-with-dimer and the tool-without-dimer configurations are minima on the potential energy surface (all positive real vibrational frequencies). The one exception is when X = C, in which case the carbene form is a shallow minimum on the PES.

Table II shows that the energy required to remove the CC dimer from the tool—the binding energy—can be selected by changing the supporting atoms. The binding energy is weakest for supporting atoms of lead. Progressing up the periodic table from lead to tin, germanium, and silicon, the binding energy of the DCB6-X dimer placement tool increases in magnitude.

Interestingly, the rising dimer binding energy weakens slightly when the supporting atoms are carbon rather than silicon. Some insight into this trend reversal at carbon may be gained by approximating the binding energy components. In Table III, the energy of the H₃X-CCH bond proxy for the energy required to break the two bonds between the carbon dimer and the supporting atoms (first column), and the energy of the H₃X-XH₃ bond acts as a proxy for the energy gained when the two supporting atoms become free to bond to each other (second column). Subtracting the second column from twice the first column as a rough proxy for the dimer binding energy (third column) gives the same trend reversal at X = C as in Table II, indicating that the increase in binding energy from Si-Si to C-C may be substantially greater than the increase from Si-CC to C-CC, paradoxically reducing the dimer removal energy for X = C.

Table II. Energy required to remove the CC dimer from the tool.

X	Energy (eV)	Level of theory
C	8.588	B3LYP/6-311 + G(2d,p)//B3LYP/3-21G*
Si	8.788	B3LYP/6-311 + G(2d,p)//B3LYP/3-21G*
SiGe	8.058	B3LYP/6-311 + G(2d,p)//B3LYP/3-21G*
Ge	7.802	B3LYP/6-311 + G(2d,p)//B3LYP/3-21G*
Sn	7.246	B3LYP/LANL2DZ//B3LYP/LANL2DZ
Pb	6.148	B3LYP/LANL2DZ//B3LYP/LANL2DZ

See footnotes of Table I for calculational details.

Table III. Proxies for the bond energy of supporting atoms on discharged tip, supporting atom to dimer, and net dimer removal energy, using a simple bond-energy model with Gaussian 98.

X	H ₃ X-CCH	H ₃ X-XH ₃	Dimer removal
C	-5.30	-3.57	-7.03
Si	-5.26	-2.99	-7.53
SiGe	—	-2.85	-7.21
Ge	-4.80	-2.78	-6.82
Sn	-4.61	-2.24	-6.98
Pb	-4.18	-1.91	-6.45

Values are in eV. See footnotes from Table I for calculational details.

It is possible that the use of the DCB6-X tool with X = Si might be problematic on some diamond surfaces, given that the X = C tool has a slightly smaller binding energy, which suggests that the dimer could remain adhered to the X = Si tool in favor of detachment. However, it is not clear that the X = C tool is a good proxy for any particular diamond surface. For example, two adjacent carbon radicals exposed on an otherwise hydrogenated diamond C(111) surface would interact only weakly. Such radicals would not behave as the two strongly interacting carbon support atoms in the X = C tool and thus should not weaken the attachment of the dimer to the C(111) surface, unlike the two supporting atoms in the X = C tool.

The energy difference between the horizontal dimer and the vertical (carbenic) forms is given in Table IV. In all cases but X = C, the carbene form is a transition state (one imaginary frequency). For X = C, the carbene form is a minimum on the PES (rather than a transition state).

A more careful investigation of the PES for the case of X = Si suggests an absence of unexpected stationary points in the immediate vicinity of the three structures already described: the horizontal dimer, the vertical dimer, and the tool without the dimer. Our expectation that the carbene (vertical dimer) rearrangement is a transition state was confirmed with frequency calculations at the higher B3LYP/6-31G* level of theory. Further analysis at the B3LYP/3-21G* level of theory starting from the vertical carbene transition state and following the eigenvector for that transition state (using the IRC keyword in Gaussian) and then minimizing showed that the two minima associated with the transition state are both the horizontal dimer form of the tool. That is, the vertical dimer carbene transition state connects two known stationary points: the

Table IV. Energy difference between the horizontal dimer and the vertical (carbene) form.

X	Energy (eV)	Level of theory
C	0.37	B3LYP/6-311 + G(2d,p)//B3LYP/3-21G*
Si	0.96	B3LYP/6-311 + G(2d,p)//B3LYP/3-21G*
Ge	0.86	B3LYP/6-311 + G(2d,p)//B3LYP/3-21G*
Sn	0.74	B3LYP/LANL2DZ//B3LYP/LANL2DZ
Pb	0.65	B3LYP/LANL2DZ//B3LYP/LANL2DZ

two horizontal dimer structures. Finally, several candidate minima structures created with MM+ in HyperChem with conceivable but unusual bonding patterns all converged to one of the three stationary points already discussed.

It is difficult to guarantee the absence of unexpected minima, and only the case of X = Si was investigated more carefully in the present study. However, it appears that the three stationary points described—the DCB6 with horizontal dimer (a minimum), the DCB6 with the vertical (carbene) dimer (a transition state), and the DCB6 without the dimer (a minimum)—define all of the relevant stationary points for X = Si, Ge, Sn, and Pb. For X = C, there is an additional transition state between the horizontal minimum and the vertical (carbene) minimum. But because the X = C structure will not be used as a tool, this latter transition state was not identified. While we cannot state with certainty that other stationary points do not exist, molecular dynamics at the AM1 level did not reveal their presence.

3.2. Singlet/Triplet Energy Gap

Beyond a more careful analysis of the stationary points of the DCB6 tools with X = Si, the singlet/triplet energy gap was also computed for this structure. Using the singlet-optimized B3LYP/3-21G* geometry for the DCB6-Si with horizontal dimer, the triplet/singlet energy gap was determined by comparing the single-point energies computed at the B3LYP/6-311+G(2d,p) level of theory without zero point correction for either the singlet or triplet energies for purposes of this comparison. Geometries were optimized at the lower level of theory in the singlet state, and the triplet single-point energy at that geometry was then computed (see Table I). The singlet state is energetically preferred to the triplet state by a substantial margin: 3.44 eV for the horizontal dimer and 2.92 eV for the vertical dimer. This large energy gap suggests that the possibility of the system being in a triplet state at room temperature from thermal activation can be neglected.

3.3. Molecular Dynamics Simulation

Ab initio molecular dynamics simulations using gradient-corrected density functional theory and a plane-wave basis (using VASP, the Vienna *Ab initio* Simulation Package)¹⁶ were carried out on the DCB6-Si dimer placement tool containing a carbon dimer attached to the two terminal silicon atoms (X = Si). The simulation, performed for 5 ps at an internal temperature of 1000 K, predicts that the horizontal dimer structure should remain stable under conditions of moderately high temperatures. A further simulation of this tool using AM1 at a temperature of 900 K for 200 ps also did not result in any rearrangements.

Of course, single trajectories for 5–200 ps are insufficient to ensure long-term stability of the dimer on

the deposition tool. As an additional check, the Arrhenius equation for the one-step thermal desorption rate $k_1 = \nu \exp(-E_d/k_B T)$ may be used to crudely approximate the canonical residence time for a CC dimer attached to a tool tip heated to temperature T .^{17,18} Taking $T = 300$ K, $k_B = 1.381 \times 10^{-23}$ J/K (Boltzmann's constant), $E_d = 6.148$ eV for the weakest tool-bound dimer (the DCB6-Pb tool, Table II), and the pre-exponential constant $\nu \sim k_B T/h \sim 6 \times 10^{12}$ s⁻¹ ($h = 6.63 \times 10^{-34}$ J-s) typically used for thermally migrating chemisorbed hydrocarbon adatoms on diamond surface^{19–24} (the precise value of which does not sensitively influence the conclusion), the lifetime of the CC dimer against spontaneous dissociation from the tool tip is $k_1^{-1} \sim 10^{90}$ s.

4. CONCLUSIONS

The DCB6-X family of dimer placement tools, for X = Si, Ge, Sn, and Pb, should be stable in a vacuum when used at room temperature, and possibly at significantly higher temperatures. The CC dimer in these structures should remain oriented horizontally with a high probability. The proposed dimer placement tools should be able to hold and position a CC dimer in a manner suitable for positionally controlled diamond mechanosynthesis at room temperature.

The CC dimer is bound to these tools by progressively weaker bonds, moving from Si to Pb, facilitating release of the CC dimer from the tool and its attachment to a growing molecular structure. The chemical reactions by which these tools interact with and deposit a CC dimer on a growing diamond surface will be investigated computationally in future work.

References and Notes

1. C. B. Musgrave, J. K. Perry, R. C. Merkle, and W. A. Goddard III, *Nanotechnology* 2, 187 (1991).
2. K. E. Drexler, *Nanosystems: Molecular Machinery, Manufacturing, and Computation*, Wiley, New York (1992).
3. R. C. Merkle, *Nanotechnology* 8, 149 (1997).
4. S. P. Walch and R. C. Merkle, *Nanotechnology* 9, 285 (1998).
5. S. B. Sinnott, R. J. Colton, C. T. White, and D. W. Brenner, *Surf. Sci.* 316, L1055 (1994).
6. D. W. Brenner, S. B. Sinnott, J. A. Harrison, and O. A. Shenderova, *Nanotechnology* 7, 161 (1996).
7. M. Page and D. W. Brenner, *J. Am. Chem. Soc.* 113, 3270 (1991).
8. M. Page and D. W. Brenner, in *Proceedings of the Second International Conference New Diamond Science and Technology*, edited by R. Messier, J. T. Glass, J. E. Butler, and R. Roy, Materials Research Society, Pittsburgh, PA (1991), p. 45.
9. X. Y. Chang, M. Perry, J. Peploski, D. L. Thompson, and L. M. Raff, *J. Chem. Phys.* 99, 4748 (1993).
10. A. Ricca, C. W. Bauschlicher, Jr., J. K. Kang, and C. B. Musgrave, *Surf. Sci.* 429, 199 (1999).
11. F. N. Dzegilenko, D. Srivastava, and S. Saini, *Nanotechnology* 9, 325 (1998).
12. IUPAC Commission on Nomenclature of Organic Chemistry, *A Guide to IUPAC Nomenclature of Organic Compounds: Table 21. Saturated Polycyclic Hydrocarbons. Type 1—Unlimited Substitution*, Blackwell Scientific, Malden, MA (1993).

13. H. F. Reinhardt, *J. Org. Chem.* 27, 3258 (1962).
14. M. J. Frisch, G. W. Trucks, H. B. Schlegel, G. E. Scuseria, M. A. Robb, J. R. Cheeseman, V. G. Zakrzewski, J. A. Montgomery, Jr., R. E. Stratmann, J. C. Burant, S. Dapprich, J. M. Millam, A. D. Daniels, K. N. Kudin, M. C. Strain, O. Farkas, J. Tomasi, V. Barone, M. Cossi, R. Cammi, B. Mennucci, C. Pomelli, C. Adamo, S. Clifford, J. Ochterski, G. A. Petersson, P. Y. Ayala, Q. Cui, K. Morokuma, P. Salvador, J. J. Dannenberg, D. K. Malick, A. D. Rabuck, K. Raghavachari, J. B. Foresman, J. Cioslowski, J. V. Ortiz, A. G. Baboul, B. B. Stefanov, G. Liu, A. Liashenko, P. Piskorz, I. Komaromi, R. Gomperts, R. L. Martin, D. J. Fox, T. Keith, M. A. Al-Laham, C. Y. Peng, A. Nanayakkara, M. Challacombe, P. M. W. Gill, B. Johnson, W. Chen, M. W. Wong, J. L. Andres, C. Gonzalez, M. Head-Gordon, E. S. Replogle, and J. A. Pople, *Gaussian 98*, Revision A.11, Gaussian Inc., Pittsburgh, PA (2001).
15. J. B. Foresman and A. Frisch, *Exploring Chemistry with Electronic Structure Methods: A Guide to Using Gaussian*, 2nd Ed., Gaussian Inc., Pittsburgh, PA (1996).
16. G. Kresse and J. Furthmüller, *Vienna Ab-Initio Simulation Package (VASP): The Guide*, VASP Group, Institut für Materialphysik, Universität Wien Vienna, Austria (2003).
17. C. Accary, P. Barbarat, W. L. Hase, and K. C. Hass, in *Proceedings of the Third International Symposium on Diamond Materials*, edited by J. P. Dismukes and K. V. Ravi, Electrochemical Society, Pennington, NJ (1993), p. 178.
18. Th. Schaich, J. Braun, J. P. Toennies, M. Buck, and Ch. Woll, *Surf. Sci.* 385, L958 (1997).
19. S. P. Mehandru and A. B. Anderson, *Surf. Sci.* 248, 369 (1991).
20. S. Skokov, B. Weiner, and M. Frenklach, *J. Phys. Chem.* 98, 7073 (1994).
21. E. J. Dawnkaski, D. Srivastava, and B. J. Garrison, *J. Chem. Phys.* 102, 9401 (1995).
22. E. J. Dawnkaski, D. Srivastava, and B. J. Garrison, *J. Chem. Phys.* 104, 5997 (1996).
23. M. Frenklach and S. Skokov, *J. Phys. Chem.* 101, 3025 (1997).
24. Y. G. Hwang and Y. H. Lee, *J. Korean Phys. Soc.* 33, 467 (1998).

Received: 9 October 2002. Revised/Accepted: 17 February 2003.